Nanocatalysts Based on Ni Nanoparticles in Functionalized Ionic Liquids for Chemoselective Hydrogenation and Transfer Hydrogenation of α,β-unsaturated Carbonyl Compounds

Deepthy Krishnan, Leonhard Schill, M. Rosa Axet, Karine Philippot, Anders Riisager

Nanocatalysts based on Ni nanoparticles in functionalized ionic liquids for chemoselective hydrogenation and transfer hydrogenation of α,β-unsaturated carbonyl compounds

Deepthy Krishnan,[a,b,c] Leonhard Schill,[a] M. Rosa Axet,[b,c] Karine Philippot,*[b,c] and Anders Riisager*[a]

[a] D. Krishnan, Dr. L. Schill, Prof. A. Riisager
Centre for Catalysis and Sustainable Chemistry, Department of Chemistry
Technical University of Denmark
DK-2800 Kgs. Lyngby, Denmark.
E-mail: ar@kemi.dtu.dk

[b] D. Krishnan, Dr. M. Rosa Axet, Dr. K. Philippot
CNRS, LCC (Laboratoire de Chimie de Coordination)
205 Route de Narbonne, BP44099, 31077 Toulouse Cedex 4
E-mail: karine.philippot@lcc-toulouse.fr

[c] D. Krishnan, Dr. M. Rosa Axet, Dr. K. Philippot
Université de Toulouse, UPS, INPT
31077 Toulouse Cedex 4, France
E-mail: karine.philippot@lcc-toulouse.fr

Abstract: For the development of catalytically active and selective Ni nanoparticle (NP) catalysts both the choice of the synthesis method and the selection of stabilizer are key parameters. A series of Ni NPs were synthesized in various ionic liquids (Ni/ILs) and applied as catalysts for the chemoselective reduction of 2-cyclohexen-1-one (**1**), as a representative of the group of α,β-unsaturated carbonyl compounds with industrial relevance. The Ni/ILs systems were found to be efficient catalysts for the selective hydrogenation of **1** to cyclohexanone (**2**) under quite mild reaction conditions (130-170°C, 10 bar H_2, **1**/Ni molar ratio of 100/1), achieving high conversions in a short reaction time (1 h). The oxidized counterparts (Ni-NiO/ILs) showed to be active for the selective catalytic transfer hydrogenation (CTH) of **1** to 2-cyclohexen-1-ol (**3**) with 2-propanol, also under mild reaction conditions (150 °C, 48 h, **1**/Ni ratio of 50/1).

Introduction

The chemoselective reduction of olefinic bonds in α,β-unsaturated carbonyl compounds is relevant for the synthesis of industrially and pharmaceutically key chemicals,[1–4] thus making it substantial to develop cost-effective and reusable catalysts for the reaction. Up to now, most catalysts used for the reduction reaction rely on metal nanoparticles (NPs) of precious metals like Ru, Ir, Rh, Pt, and Pd,[1,2,5,6] but few NPs based on abundant metals like Fe, Co and Ni have also been advantageously employed, offering cheaper catalysts.[7,8] Particularly, Ni NPs are also known as attractive catalysts for other important catalyzed organic reactions like alkylation of ketones,[9] transfer hydrogenation of alkenes/carbonyl compounds,[8] semi-alkyne hydrogenation[10] and reductive amination of aldehydes.[8]

Well-defined Ni NPs can be generated in solution by the reduction of a nickel(II) salt, *e.g.* nickel(II) chloride ($NiCl_2$) with lithium and 4,4′-di-*tert*-butylbiphenyl (DTBB) as stabilizer,[11,12] or the reduction of nickel(II) acetate ($Ni(OAc)_2$) with aqueous hydrazine.[13] Also, nickel(II) bis(acetylacetonate) ($Ni(acac)_2$) can be used to synthesize size-tunable Ni NPs through thermal decomposition in the presence of *n*-trioctylphosphine as a capping ligand and alkylamines as a size-limiting agent.[14] An alternative and efficient method to obtain size-controlled Ni NPs in solution relies on the decomposition of an organometallic complex like bis(η^4-1,5-cyclooctadiene)nickel(0) ($[Ni(COD)_2]$)[15–17] under hydrogen in the presence of different stabilizing agents.[15,18] This organometallic approach is especially attractive as it allows fine control of the growth of the NPs, while offering a clean metal surface due to the absence of by-product.[19] Philippot and coworkers[18] have synthesized a series of Ni NPs with similar mean size (*ca*. 5-6 nm) from $[Ni(COD)_2]$ and different stabilizers (*e.g.*, polyvinylpyrrolidone, hexadecylamine, octanoic acid and stearic acid), and applied these NPs for the chemoselective hydrogenation of α,β-unsaturated carbonyl compounds like cinnamaldehyde, cinnamic acid, *trans*-chalcone, *etc.* under mild reaction conditions (THF, 4 bar H_2, 60 °C). All the Ni nanocatalysts selectively hydrogenated the olefinic bond, which was attributed to a high content of Ni^0 in the NPs as evidenced from characterization by extended X-ray absorption fine structure (EXAFS) and X-ray photoelectron spectroscopy (XPS). However, the carboxylic acid-stabilized Ni NPs exhibited superior activity compared to the other Ni NPs, thus indicating that the nature of the stabilizer strongly affected the catalytic properties of the Ni nanocatalysts.

The synthesis of Ni NPs can also be completed in ionic liquids (ILs), where the ILs are used as both stabilizers and dispersion media. Using this approach, Jiang *et al.*[20] synthesized Ni NPs (mean size 5.1 nm) in 1-butyl-2,3-dimethylimidazolium (*S*)-2-pyrrolidinecarboxylic acid IL by the reduction of $Ni(OAc)_2$ with $NaBH_4$ or hydrazine and applied these Ni NPs for the chemoselective hydrogenation of quinoline and aromatic nitro compounds. Likewise, Dupont and coworkers[21] synthesized Ni NPs in 1-alkyl-3-methylimidazolium bis(trifluoromethanesulfonyl)-imide ILs (alkyl = butyl to hexadecyl) with the organometallic approach by decomposing $[Ni(COD)_2]$ under hydrogen pressure

(4 bar). They observed that ILs with a longer alkyl side chain induced the formation of Ni NPs with a smaller diameter and a narrower size distribution (4.9 ± 0.9 to 5.9 ± 1.4 nm). They employed the Ni NPs dispersed in 1-butyl-3-methylimidazolium bis(trifluoromethanesulfonyl)imide IL in the catalytic hydrogenation of cyclohexene. A related approach for the synthesis of Ni NPs in imidazolium ILs has been reported by Prechtl, Santini, Dupont and coworkers[22] in which the imidazolium ILs acted not only as a solvent and a stabilizer but also as a promoter for the auto-decomposition of the $[Ni(COD)_2]$ under mild reaction conditions. This method has the advantage of not using any reducing agent, thus easing the procedure and limiting the contamination of the NPs that may happen with $NaBH_4$ or hydrazine. Prechtl and coworkers[23] also followed this approach to synthesize a series of Ni NPs (size range: 4.4 ± 0.7 to 8.3 ± 1.6 nm) in nitrile-functionalized imidazolium based ILs (CN-FILs) with different alkyl chain length and substitution at the C_2 position of the imidazolium cation. The obtained Ni NPs catalyzed the semi-hydrogenation of alkynes to (*Z*)-alkenes at near ambient conditions as well as the selective hydrogenation of benzonitrile to benzylamine.[24] Moreover, Ni NPs stabilized by alkaline poly(1-vinyl-3-alkyl-imidazolium) hydroxide ILs (alkyl = ethyl, butyl or pentyl) were synthesized by Vijayakrishna *et al.*[25] and found to be durable catalysts for the catalytic transfer hydrogenation (CTH) of α,β-unsaturated carbonyl compounds like acetophenone, benzophenone, cyclohexanone*, etc.* with 2-propanol as H-donor and solvent under mild reaction conditions (80 °C, substrate/Ni ratio of 10/1). Notably, the trend in catalytic activity also followed the alkyl chain length of the IL.

Besides Ni NPs, ILs have also been used as reaction media to synthesize NiO NPs in 1-butyl-3-methylimidazolium triflate by the reduction of nickel(II) nitrate hexahydrate ($Ni(NO_3)_2{\cdot}6H_2O$) with NaOH followed by calcination.[26] These NiO NPs were found to exhibit superparamagnetic behavior although NiO as bulk material is antiferromagnetic, but the Ni NPs were not applied for catalysis. However, Riisager and coworkers[27] have shown that commercial NiO NPs (size *ca.* 15 nm) as well as synthesized 3D nano-/micrometer-scaled NiO materials with urchin-like structure[28] are highly efficient and reusable catalysts for CTH of carbonyl compounds (*e.g.*, biomass-derived furfural) using 2-propanol as H-donor and solvent under mild conditions (120-150 °C, 3-4 h). These latter results suggest that NiO NPs-IL systems may also be active for the transfer hydrogenation catalysis.

In this work, novel Ni NPs and Ni-NiO NPs were synthesized by the organometallic approach, from $[Ni(COD)_2]$, in the two ether-FILs 1-methoxyethoxy-methyl-3-methylimidazolium bis(trifluoromethanesulfonyl)imide, $[MEMIm][NTf_2]$ or MEM, and 1-methoxymethoxyethyl-3-methylimidazolium bis(trifluoromethanesulfonyl)imide, $[MMEIm][NTf_2]$ or MME, and characterized. The choice of FILs was inspired by the literature data which evidence that methoxy functionality can lead to well dispersed and highly active metal NPs for catalysis. Thus, numerous examples of metal NPs can be found in the literature that have been synthesized using polyethylene glycol (PEG) as stabilizer and that have shown high catalytic activity in several reactions.[29–32] Given that, our concept entailed to combine the stabilization effect of the methoxy group and the versatile nature of the ILs by synthesizing imidazolium ILs incorporating the methoxy functionality. The two Ni NPs/FIL systems, Ni/MEM and Ni/MME, were applied for the hydrogenation of 2-cyclohexen-1-one (**1**) with the aim to probe the surface reactivity in terms of conversion and selectivity. Two other systems of Ni NPs dispersed in either the non-functionalized IL 1-hexyl-3-methylimidazolium bis(tri-fluoromethanesulfonyl)imide (Ni/H) or in the nitrile-FIL 1-butylcyano-3-methylimidazolium bis(trifluoromethanesulfonyl) imide $[(CH_3CH_2CH_2CH_2CN)MIm][NTf_2]$ (Ni/CN) were also synthesized for the purpose of comparison. In a second stage, the as-synthesized Ni/ILs NPs were oxidized to Ni-NiO/ILs NPs and applied for the CTH of **1** with 2-propanol.

Experimental Section

General methods and materials

All operations for the synthesis of Ni/IL NPs and the catalytic reactions were performed under inert atmosphere (argon) using standard Schlenk techniques or in a glovebox (MBraun). Pentane, acetonitrile (MeCN), acetone, dichloromethane (DCM) and diethyl ether were purified by standard methods or using a MBraun SPS-800 solvent purification system, and further degassed using the freeze-pump thaw technique or argon bubbling. All ILs were prepared according to procedures described previously.[33] 2-Cyclohexen-1-one (**1**; >95%, Sigma Aldrich), cyclohexanone (**2**; ≥99%, Sigma Aldrich), 2-cyclohexen-1-ol (**3**; 95%, Sigma Aldrich), cyclohexanol (**4**; 99%, Sigma Aldrich), $[Ni(COD)_2]$ (>98%, Strem Chemicals), H_2 (99.999%, Air Liquid) and argon (99.99%, Air Liquid) were use as received.

Catalyst preparation

In a typical reaction, $[Ni(COD)_2]$ (16.27 mg, 0.06 mmol) was dissolved in pentane (1 mL) and IL (3 mL) in a Fischer-Porter bottle, whereafter the solution was stirred (1500 rpm) for 24 h at 80 °C using a magnetic stirrer. Then, the generated cyclooctane was removed under vacuum (≈0.05 mbar) and the resultant black colloidal suspension containing Ni NPs stored under argon.

Ni-NiO/ILs were obtained by oxidizing the corresponding Ni/FILs. The colloidal suspensions of Ni/ILs were placed in closed 20 mL vials at room temperature and subjected to three different oxidative treatments: exposure to static air for 24 h under stirring (200 rpm) (oxidation treatment 1 – OT_1), exposure to static air for 20 days without stirring (oxidation treatment 2 – OT_2), or exposure to air continuously passed through the suspension for 0.5 h without stirring (oxidation treatment 3 – OT_3).

Catalyst characterization

Transmission electron microscopy (TEM) and high-resolution transmission electron microscopy (HRTEM) analyses (Centre de microcaractérisation Raimond Castaing, CNRS-UAR 3623, Toulouse) were performed on a JEOL JEM 1011 CXT electron microscope operating at 100 kV with a point resolution of 4.5 Å or a JEOL JEM 1400 operating at 120 kV with a point resolution of 2.0 Å, and on a JEOL JEM 2100F equipped with a field emission

gun (FEG) operating at 200 kV with a point resolution of 2.3 Å, respectively. High-angle annular dark-field scanning transmission electron microscopy (HAADF-STEM) was performed on a JEOL JEM-ARM200F Cold FEG operating at 200 kV with a point resolution of >1.9 Å. The TEM samples were prepared by diluting a few drops of each Ni/FIL and Ni-NiO/FIL in MeCN and casting a drop of this solution on a carbon-coated copper grid. Size distributions and mean sizes of the NPs were determined by measurement of at least 200 individual NPs on a given grid using the software ImageJ.

XPS analyses were performed using a Thermo Scientific system at room temperature using AlKα radiation (1484.6 eV) and a spot size of 400 µm. A flood gun was used to reduce sample charging effects and the obtained spectra were further corrected by setting the C 1s binding energy at 284.8 eV. Data processing was done using the Avantage 4.87 software.

Metal content was determined by inductively coupled plasma optical emission spectroscopy (ICP-OES) using a Thermo Scientific ICAP 6300 instrument.

Catalytic hydrogenation

Hydrogenation of 2-cyclohexen-1-one (**1**) was carried out in a 20 mL stainless steel high-pressure batch reactor. In a standard experiment, **1** (0.1 mL, 1 mmol) was placed into a vial containing Ni/ILs or Ni-NiO/ILs (0.01 mmol of metal) and octane (0.05 mL, 0.3 mmol; internal standard). The vial was positioned into the reactor which was then purged three times with H_2 and subsequently pressurized with H_2 (10 bar). To avoid external mass transfer limitation, a stirring of 1200 rpm was applied at the desired temperature for the indicated reaction time. Six different sets of mixtures containing the same substrate/catalyst ratio and internal standard were prepared and converted at the mentioned reaction conditions. Each reaction was stopped at different intervals of time for quantitative gas chromatography (GC) analysis to determine the catalytic performance.

Catalyst recycling was performed using the Ni/FILs systems at 130 °C following the procedure described above. The spent catalytic phase was washed with pentane (3 × 5 mL) after each catalytic run to remove substrate and formed products, followed by drying under vacuum (≈0.05 mbar) at room temperature for 1 h. The dried catalytic phase was then mixed with a new batch of **1** and the next reaction performed under identical conditions. This operation was repeated five times. TEM analysis was performed on the spent catalysts after the last catalytic runs.

Catalytic transfer hydrogenation (CTH)

The CTH of 2-cyclohexen-1-one (**1**) was performed in a ACE pressure tube (Ace-Thred 15 PTFE front-seal plug, 15 mL, Sigma Aldrich) equipped with magnetic stirrer and oil bath. In a typical reaction, **1** (0.1 mL, 1 mmol), Ni-NiO/ILs catalyst (0.02 mmol of metal), 2-propanol (5 mL; H-donor and solvent) and decane (0.06 mL, 0.3 mmol; internal standard) were mixed in a reactor. After sealing, the reactor was placed in a preheated oil bath (150 °C) for 48 h under stirring (600 rpm). Aliquots of the reaction mixture were taken at different intervals of time for quantitative GC analysis to determine the catalytic performance.

Product analysis from catalytic reactions

Quantitative determination of the product mixtures from the catalytic reactions was performed by GC analysis with flame ionization detection (FID) using the internal standard method with calibration curves built with commercial references on an Agilent 6850-5975C GC equipped with HP-5MS capillary column (30.0 m × 250 µm × 0.25 µm) and He carrier gas (He flow: 1.25 mL/min; injector temperature: 250 °C; detector (FID) temperature: 250 °C; oven program: 27 °C (hold 3 min) to 180 °C at 10 °C/min (hold 10 min) for a total run time of 26 min. Retention times: octane - 4.1 min; decane - 7.2 min; **4** - 5.5 min; **3** - 5.6 min; **2** - 5.8 min; **1** - 6.2 min).

Solubility tests in ILs

The solubility of **1** in the different ILs was evaluated by mixing IL (0.5 mL) and **1** (2 mL) under stirring at room temperature for 24 h in a vial after allowing to settle for 0.5 h.

Results and Discussion

Synthesis and characterization of Ni nanocatalysts

The Ni NPs were synthesized following slight modifications to a previously described procedure[34] by dissolving the $[Ni(COD)_2]$ precursor in a pentane/IL mixture and heating the mixture at 80 °C for 24 h under vigorous stirring (Scheme 1). This led to the formation of black colloidal suspensions with the four ILs, indicating the successful decomposition of the Ni precursor. The generated cyclooctane and pentane were removed under vacuum (≈0.05 mbar) overnight. The metal content of each Ni/IL sample was measured by ICP analysis to be *ca.* 0.10 wt.% Ni (Table 1).

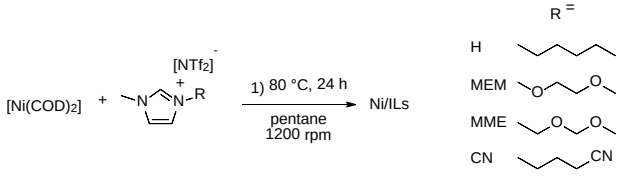

Scheme 1. Synthesis of Ni/ILs.

Table 1. Characteristics of the synthesized Ni/ILs.

Ni/ILs	Ionic liquid	Ni content (wt.%) [a]	Ni NP mean size (nm) [b]
Ni/H	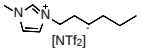	0.11	5.6 ± 0.3
Ni/MEM	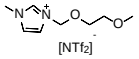	0.12	4.4 ± 0.4
Ni/MME	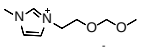	0.11	6.5 ± 0.3
Ni/CN	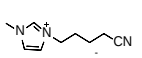	0.11	2.8 ± 0.3

[a] Determined by ICP analysis. [b] Determined from TEM analysis.

TEM analyses evidenced the formation of well-dispersed Ni NPs in the four ILs with mean sizes ranging from 2.8 to 6.5 nm

depending on the IL used (Table 1). Additionally, the morphology and the dispersion of the NPs varied with the nature of the IL as visible on the TEM images in Figure 1 (HRTEM and HAADF-STEM images are given in SI, Figures S1-S4). With a mean diameter of 2.8 nm, the CN-type FIL led to the smallest Ni NPs whereas the two ether-FILs (MEM and MME) provided in both cases larger sized Ni NPs with a difference of *ca.* 2 nm between them (4.4 and 6.5 nm, respectively) and the non-functionalized IL gave rise to Ni NPs of 5.6 nm average size. Hence, the size of the NPs followed the increasing order: Ni/CN < Ni/MEM < Ni/H < Ni/MME.

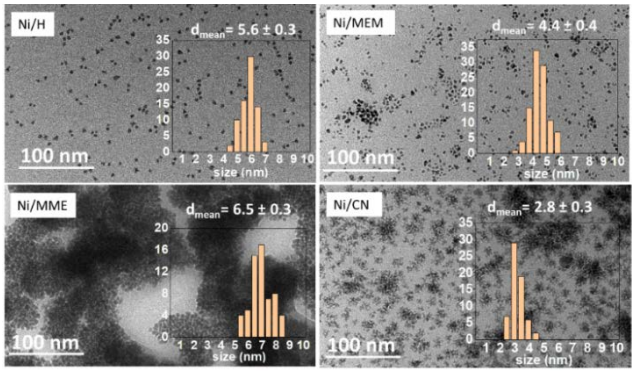

Figure 1. TEM images of the Ni/ILs with their corresponding size distributions (scale bar = 100 nm).

XPS analyses were performed on all the Ni/ILs systems and the survey spectra for each system and the deconvoluted high-resolution scan spectra of the different elements (C 1s, N 1s, F 1s, S 2p, O 1s) are compiled in SI (Figures S5-S8). The binding energies (E_b), atomic ratio (%) and the full width at half maximum FWHM (eV) of the C 1s and N 1s, O 1s, S 2p and F 1s of the Ni/ILs are also given in SI (Tables S1 and S2). Despite the very low concentration of Ni NPs in the ILs, an increased number of scans enabled acquiring Ni $2p_{3/2}$ spectra (Figure 2) which indicated the presence of both metallic Ni^0 and Ni^{2+} species. The binding energy of the metallic Ni^0 for all ILs was found at 852.16 eV which agrees with literature data.[17,35,36] The relative amounts of Ni^0 out of the total Ni content in the H, MEM, MME, CN ILs were found to be 55, 52, 51 and 60%, respectively (SI, Table S3). Considering that the determined Ni^0 contents are only related to the surface layers of the NPs, these results suggest that the surface of the Ni NPs mostly comprised metallic Ni.

The oxidation of the Ni/ILs was studied because several literature reports point to the benefit of the co-existence of Ni and NiO species for catalysis, including hydrogenation reactions.[37–40] For this purpose, fresh samples of the four Ni/ILs were exposed to air for 24 h (OT_1). TEM analyses of the so-oxidized Ni-NiO/ILs were performed to determine if the NPs underwent any change of size or/and morphology or/and dispersion during the air treatment, but no significant difference in the NP size nor morphology and dispersion was observed by TEM (Figure 3).

XPS analyses were also performed on all Ni-NiO/ILs (OT_1), which showed similar spectra to those of the ILs and Ni/ILs systems and the deconvoluted high-resolution scan spectra of the different elements (C 1s, N 1s, F 1s, S 2p, O 1s) are compiled in SI (Figures S9-S12). Also, the binding energies (E_b), atomic ratio (%) and the full width at half maximum FWHM (eV) of the C 1s and N 1s, O 1s, S 2p and F 1s of the Ni/ILs are also given in SI (Tables S4 and S5). Note that care was taken to minimize extra oxidation during sample introduction into the XPS instrument. Ni $2p_{3/2}$ high-resolution XPS scan spectra of the oxidized samples are presented in Figure 4 and show the presence of both metallic Ni^0 and Ni^{2+} species. For the H and CN ILs, no significant change in Ni^0 content was observed after exposure to air, whereas the relative concentration of metallic Ni decreased by approximately 10% for the MEM and MME systems (SI, Table S6). This might indicate that the rate of oxidation of the NPs is different depending on the nature of the IL, being slower in the presence of CN FIL compared to the MEM and MME FILs. The fact that the Ni NPs consisted of *ca.* 40-60% of metallic Ni^0 despite exposure to air yields interesting information about their stability in air. This can be an advantage for their storage and handling in catalysis.

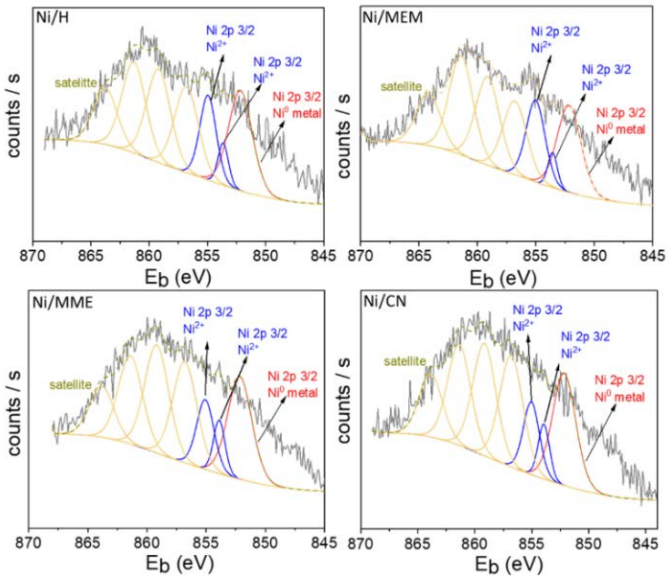

Figure 2. High-resolution XPS scan spectra of Ni 2p for the Ni/ILs.

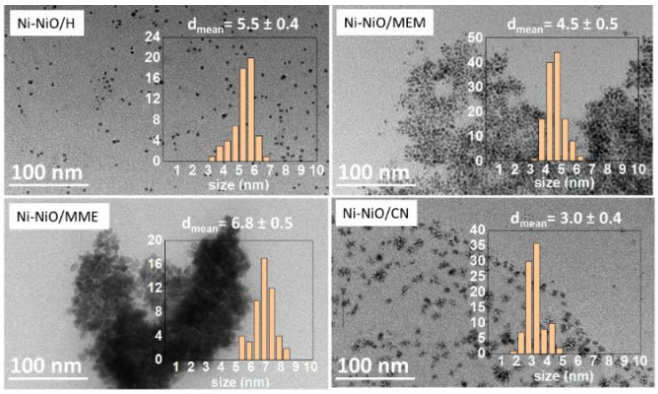

Figure 3. TEM images of Ni-NiO/ILs (OT_1) with their corresponding size distributions (scale bar = 100 nm).

To study the stability of the Ni/ILs NPs when exposed to air for a long term, the four systems were also exposed to static air for 20 days whereafter TEM images of the resulting Ni-NiO/ILs (OT_2) systems were recorded (Figure 5). It can be observed that the

NPs in the oxidized Ni-NiO/H (OT_2) system were strongly agglomerated (average size *ca*. 6.8 nm), while comparatively, the NPs in the Ni-NiO systems with MEM, MME and CN FILs remained well-dispersed after 20 days in air with an unchanged size compared to the non-oxidized Ni/ILs counterparts These results indicate that the Ni NPs synthesized in MEM, MME and CN FILs are more stable under air than when synthesized in non-functionalized H IL, suggesting that the methoxy and nitrile groups from the ILs interact stronger with the Ni NP surface and hereby provide better stabilization.

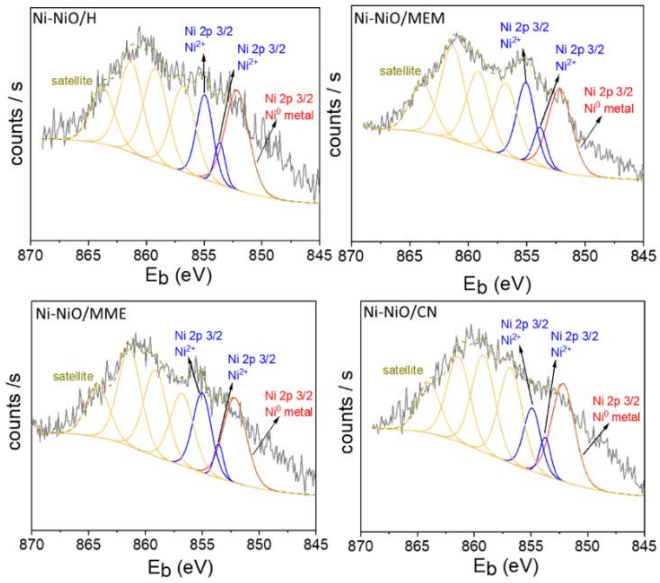

Figure 4. High-resolution XPS scan spectra of Ni 2p for the Ni-NiO/ILs.

Catalytic hydrogenation of 2-cyclohexen-1-one

The catalytic performances of the Ni/ILs and Ni-NiO/ILs (OT_1) systems were investigated for the hydrogenation of 2-cyclohexen-1-one (**1**) under relatively mild reaction conditions (130 °C, 10 bar H_2, 1 h, **1**/Ni ratio of 100/1) (Scheme 2) and the results are compiled in Table 2. A comparison of the conversion with time as the function of the Ni/ILs systems is further provided in Figure 6. Both the Ni/ILs and Ni-NiO/ILs (OT_1) systems were active and highly selective for the catalytic hydrogenation of **1** to **2** (*i.e.*, superior selectivity towards C=C hydrogenation in the presence of C=O) providing conversions between 78 and 99% in a short reaction time (1 h). The initial turnover frequencies (TOFs), calculated for the Ni/ILs systems at 0.25 h, showed some differences depending on the IL. The Ni/MEM catalyst showed the highest TOF (814 h^{-1}) followed by the Ni/CN catalyst and the Ni/H catalyst (TOFs of 712 and 677 h^{-1}, respectively). The Ni/MME catalyst, with the largest sized NPs (ca. 6.5 nm) of the series, showed the lowest TOF (627 h^{-1}). Nevertheless, all the systems showed high activity at the applied reaction conditions with an initial order of activity: Ni/MME < Ni/H < Ni/CN < Ni/MEM. Notably, solubility tests of **1** in the different ILs revealed full solubility of the substrate in all the ILs (SI, Figure S13), thus ruling out that the dependency of the activity trend observed was related to a solubility difference of the substrate. The catalytic reaction medium containing Ni/IL, **1** and octane (internal standard) also formed a monophasic system.

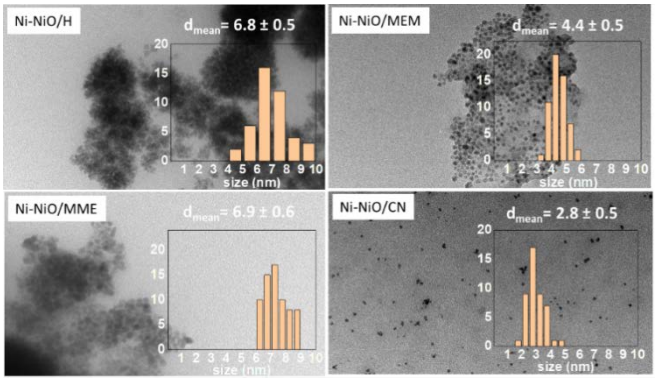

Figure 5. TEM images of Ni-NiO/ILs (OT_2) (after exposure under static air for 20 days) with their corresponding size distributions (scale bar = 100 nm).

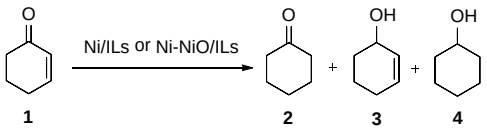

Scheme 2. Ni/ILs and Ni-NiO/ILs (OT_1) catalyzed hydrogenation of 2-cyclohexen-1-one (**1**).

Table 2. Hydrogenation of 2-cyclohexen-1-one (**1**) with Ni/ILs and Ni-NiO/ILs catalysts.[a]

Catalyst system	Conversion (%) [b]	Selectivity (%) [b]			TOF (h^{-1}) [c]
		2	**3**	**4**	
Ni/H	>99	97	0	3	677
Ni-NiO/H (OT_1)	>99	98	0	2	-
Ni/MEM	98	>99	0	0	814
Ni-NiO/MEM (OT_1)	78	>99	0	0	-
Ni/MME	>99	>99	0	0	627
Ni-NiO/MME (OT_1)	89	>99	0	0	-
Ni/CN	>99	>99	0	0	712
Ni-NiO/CN (OT_1)	>99	>99	0	0	-

[a] Reaction conditions: 0.01 mmol of Ni, 1 mmol of 2-cyclohexe-1-none (**1**), 0.3 mmol of octane (internal standard), 130 °C, 10 bar H_2, 1 h, 1200 rpm. [b] Determined by GC using internal standard technique. [c] TOF values (calculated at 0.25 h) are given based on the number of Ni surface atoms calculated from the average NPs sizes determined by TEM (SI, Table S8).

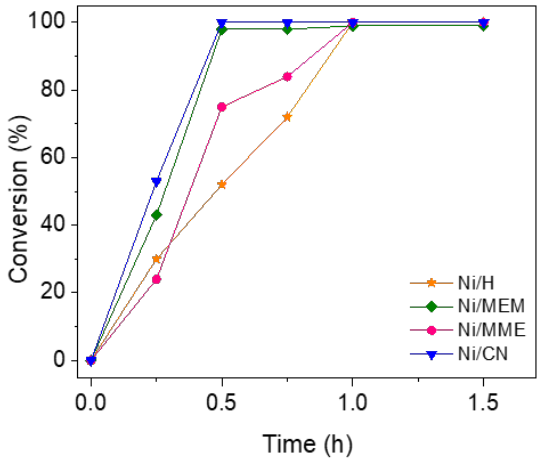

Figure 6. Time-conversion curves for the hydrogenation of 2-cyclohexen-1-one (**1**) with the different Ni/ILs catalysts. Reaction conditions: 0.01 mmol of Ni, 1 mmol of **1**, 0.3 mmol of octane (internal standard), 10 bar H_2, 130 °C, 1200 rpm.

To assess the potential impact of temperature variation on catalyst selectivity, the hydrogenation of **1** was also performed at 150 and 170 °C with the four Ni/ILs catalysts, while keeping all the other parameters constant (SI, Table S7). Under these conditions a full conversion of **1** was also observed, but interestingly, with no hydrogenation of the carbonyl group, thus indicating that even at a temperature up to 170 °C the Ni/IL catalysts are very selective towards the hydrogenation of the olefinic bond of **1**.

The hydrogenation of **1** with the oxidized Ni-NiO/ILs (OT_1) systems was also performed with the same reaction conditions as with the Ni/ILs analogues (Table 2). For Ni-NiO/MEM (OT_1) and Ni-NiO/MME (OT_1), the conversion decreased from 97 to 78% and from 99 to 89%, respectively, compared to their non-oxidized counterparts, whereas the Ni-NiO/CN (OT_1) and Ni-NiO/H (OT_1) systems did not show inferior activity in comparison to their non-oxidized analogues. The reason behind this difference in catalytic behavior could be a lower oxidation of the NP surface during air exposure when stabilized in H and CN IL, making these catalysts still active compared to the two methoxy-functionalized IL catalysts. This hypothesis is supported by the XPS data. It is noteworthy that no change in selectivity was observed after the oxidation of the four Ni/ILs catalysts, being still quantitative towards the formation of **2**. This could be due to the reduction of the Ni-NiO surface to Ni^0 upon the treatment of 10 bar of H_2 pressure applied during the catalysis, thus regenerating the active Ni surface and leading to a similar selectivity. XPS analysis of one of the oxidized catalytic systems (Ni-NiO/MEM) after catalysis showed an increase in the metallic Ni^0 to 59% which further supported the above hypothesis (SI, Figure S14).

The recyclability of the Ni/ILs catalysts for **1** hydrogenation was tested in five successive catalytic runs at 130 °C with partial conversion (0.25 h), thus providing a realistic evaluation of the catalytic performance and allowing to easily identify a decrease in catalytic activity if any (Figure 7). The Ni/FILs were found to maintain a similar **1** conversion during reuse for five reaction runs. Conversely, the **1** conversion with the Ni/H system remained only constant up to three catalytic runs but decreased in the fourth and fifth runs, pointing to a less stable system compared to its functionalized counterparts. TEM images of the spent catalyst showed that Ni/H NPs had formed agglomerates with an increase in the size of the NPs from 5.6 to 6.8 nm after the fifth reaction run, whereas the NPs in the Ni/MEM system retained their morphology with a small increase in size from 4.4 to 5.1 nm. For the Ni/MME (6.1 ± 0.8 nm) and Ni/CN (3.1 ± 0.3 nm) systems, the size of the NPs remained similar after five reaction runs (SI, Figure S15).

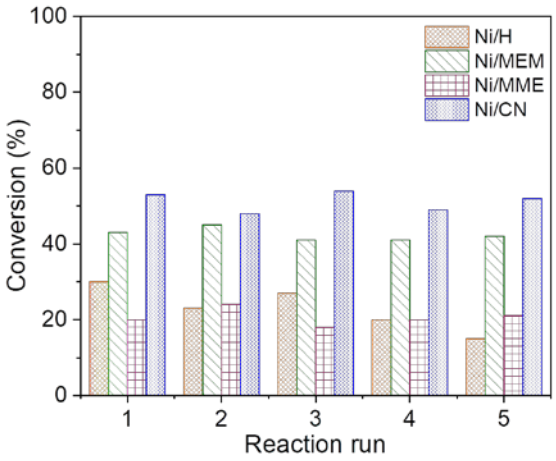

Figure 7. Recycling tests of the Ni/ILs catalysts in the hydrogenation of 2-cyclohexen-1-one (**1**). Reaction conditions: 0.01 mmol of Ni, 1 mmol of **1**, 0.3 mmol of octane (internal standard), 10 bar H_2, 130 °C, 0.25 h, 1200 rpm.

Catalytic transfer hydrogenation of 2-cyclohexen-1-one

Previous literature reports have demonstrated that NiO NPs are active for CTH of various carbonyl compounds using 2-propanol as H-transfer agent[27,28] and Ni-NiO/ILs (OT_3), *i.e.* oxidized by bubbling air through the colloidal dispersions of the Ni/ILs for 0.5 h (to ensure an uniform procedure for oxidizing the Ni/ILs systems), were therefore tested for the CTH of **1**. The Ni $2p_{3/2}$ high-resolution XPS scan spectra of the Ni-NiO/ILs (OT_3) catalysts are presented in SI (Figure S16). In general, these catalysts contained more Ni^{2+} species than their Ni-NiO/ILs (OT_1) analogues, indicating that the bubbling of air for 0.5 h resulted in improved oxidation compared to the exposure to static air for 24 h (OT_1 conditions) (SI, Table S9). Nevertheless Ni^0 was still present in all catalysts (42-60%) and the Ni-NiO/CN (OT_3) remained the less oxidized catalyst. The results from the CTH of **1** in 2-propanol at 150 °C are shown in Table 3 and Figure 8.

Table 3. CTH of 2-cyclohexen-1-one (**1**) with Ni-NiO/ILs (OT_3) catalysts.[a]

Catalyst system	Conversion (%) [b]	Selectivity (%) [b]			TOF (h^{-1}) [c]
		2	**3**	**4**	
Ni-NiO/H (OT_3)	10	0	97	3	0.2
Ni-NiO/MEM (OT_3)	73	0	>99	0	1.8
Ni-NiO/MME (OT_3)	39	0	96	4	0.7
Ni-NiO/CN (OT_3)	20	0	>99	0	0.3

[a] Reaction conditions: 0.02 mmol of Ni, 1 mmol of 2-cyclohexe-1-none (**1**), 0.3 mmol of decane (internal standard), 150 °C, 5 mL 2-propanol, 48 h, 600 rpm. [b] Determined by GC using internal standard technique. [c] TOF calculated as mol of **1** converted per mol of Ni per h after 10 h.

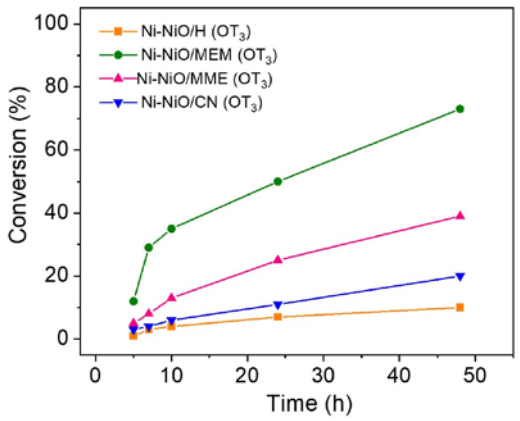

Figure 8. Time-conversion curves for the CTH of 2-cyclohexen-1-one (**1**) with Ni-NiO/ILs (OT_3) catalysts. Reaction conditions: 0.02 mmol of Ni, 1 mmol of **1**, 0.3 mmol of decane (internal standard), 5 mL 2-propanol, 150 °C, 600 rpm.

The four oxidized Ni-NiO/ILs (OT_3) systems were active for the CTH of **1**, yielding conversions between 10 and 73% after 48 h of reaction. Interestingly, the oxidized Ni/MEM and Ni/CN systems selectively formed **3** (>99%), while oxidized Ni/H and Ni/MME systems showed a slightly lower selectivity (Table 3). These results emphasize that the systems had very different reaction rates for the CTH of olefinic and carbonyl groups depending on the ILs. The overall CTH TOFs were calculated for the catalysts after 10 h. A comparison of the catalytic performances with time confirmed the order of CTH reactivity to: Ni/H < Ni/CN < Ni/MME < Ni/MEM (Figure 8). A Ni/MEM catalyst has been further used for CTH of the substrate 1 under the same reaction conditions (150 °C, 48 h, substrate/Ni ratio of 50/1). A 58% conversion was achieved which was lower than the conversion observed for the oxidized system Ni-NiO/MEM (78%). When the Ni/MEM was treated under 10 bar hydrogen at 150 °C for 12 h and then employed for the CTH reaction, a slightly lower conversion of 50% was obtained. The decrease in conversion may indicate that the active species for the CTH is the NiO and that the conversion depends on the content of NiO present on the surface of the Ni NPs.

The difference in hydrogenation reactivity of the non-oxidized and the oxidized catalysts toward the olefinic and carbonyl groups of **1** is possibly caused by a preference for adsorption of carbonyl groups on the surface of the oxidized catalysts, as illustrated in Figure 9. In the oxidized systems, Ni^{2+} and O^{2-}/OH^- sites on the surface of the Ni NPs can act as acidic and basic sites, respectively, with the sites preferentially adsorbing the C=O group due to its amphoteric nature. These strong interactions have also been deduced from theoretical calculations.[41] As previously described,[27,28] the activation of 2-propanol during CTH may occur on the catalyst surface with simultaneous adsorption and activation of the C=O group, and the hydrogen transfer proceeding *via* a cyclic intermediate between 2-propanol and **1**. Conversely, adsorption of hydrides occurs preferentially onto the metallic Ni^0 surface under H_2 atmosphere. As a result, the reaction selectivity in the presence of H_2 is mainly governed by these surface hydrides,[42] favoring the hydrogenation of the olefinic bond over the carbonyl group.

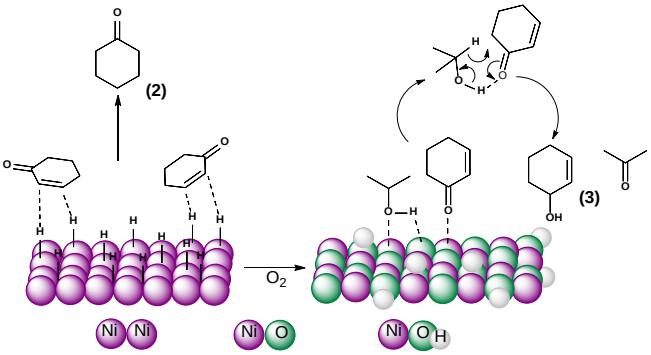

Figure 9. Schematic representation of the possible adsorption of reactants with the Ni/ILs catalysts (left) and Ni-NiO/ILs catalysts (right) during **1** hydrogenation and CTH, respectively.

Conclusion

A series of catalysts based on Ni NPs dispersed in a non-functionalized IL (H) and three functionalized ILs containing nitrile- (CN) and methoxy-groups (MEM and MME) have been synthesized, characterized, and applied in the hydrogenation of **1**. The Ni/MEM and Ni/MME catalysts were novel systems of Ni NPs, whereas the Ni/H and Ni/CN were previously reported and here prepared for comparison purpose. It is noteworthy that smaller Ni NPs were obtained for the Ni/CN system (2.8 nm) compared to previous literature reports (7-8 nm).[24] All the Ni/ILs systems were found to be efficient catalysts for the chemoselective hydrogenation of **1** to **2** under mild reaction conditions (130-170°C, 10 bar H_2, **1**/Ni ratio of 100/1), achieving high conversions in a short reaction time with a reactivity order: Ni/H < Ni/MME < Ni/CN < Ni/MEM. Compared to literature results using Ni NPs synthesized in amine-functionalized ILs,[43] good catalytic performance was achieved with much less Ni metal content under neat conditions. Aerobically oxidized Ni/ILs systems were also

found to be moderately active for the hydrogenation of the olefinic bond of **1**, thus highlighting a good stability of the catalysts despite the small NP size. Furthermore, the oxidized catalysts showed to be active for the selective CTH of **1** to **3** with 2-propanol under mild reaction conditions (150 °C, 48 h, **1**/Ni ratio of 50/1) with a reactivity order: Ni/H < Ni/CN < Ni/MME << Ni/MEM, which is different from the hydrogenation reaction. Compared to earlier reports using substrate/Ni ratios between 5/1 and 33/1,[25,44] the present work uses much less Ni metal while providing a higher conversion in 48 h. Remarkably, this work illustrates how the tailoring of the surface oxidative state of Ni/ILs catalysts and the use of either H_2 or 2-propanol as hydrogen source can be a strategy for chemoselective reduction of an α,β-unsaturated carbonyl compound to different products of industry relevance. The selectivity difference likely originates from unlike coordination mechanisms of the substrate onto the catalyst surface, being surface Ni species and hydrides present at the surface, and in perspective this distinction may also be transferable to the reduction of other unsaturated substrates.

Acknowledgements

This work has received funding from the European Union's Horizon 2020 research and innovation program under the Marie Skłodowska-Curie grant agreement No. 860322 (CCIMC project). The authors thank Technical University of Denmark, CNRS and Université Fédérale de Toulouse-Paul Sabatier for support and V. Colliere (CNRS) for help with the TEM analyses.

Conflict of Interest

The authors declare no conflict of interest.

Keywords: functionalized ionic liquid • nickel nanoparticles • chemoselective catalysis • hydrogenation • catalytic transfer hydrogenation • α,β-unsaturated carbonyl compounds

[1] A. Nagendiran, V. Pascanu, A. Bermejo Gómez, G. González Miera, C. W. Tai, O. Verho, B. Martín-Matute, J. E. Bäckvall, *Chem. Eur. J* **2016**, *22*, 7184–7189.

[2] S. Doherty, J. G. Knight, T. Backhouse, E. Abood, H. Alshaikh, I. J. S. Fairlamb, R. A. Bourne, T. W. Chamberlain, R. Stones, *Green Chem.* **2017**, *19*, 1635–1641.

[3] E. Keinan, N. Greespoon *In Comprehensive Organic Synthesis*, Vol. 8 (Eds.: B. M. Trost, I. Fleming), Pergamon, Oxford, **1991**.

[4] F. Alonso, G. Radivoy, M. Yus, *Russ. Chem. Bull.* **2003**, *52*, 2563–2576.

[5] M. Serhan, D. Jackemeyer, M. Long, M. Sprowls, I. Diez Perez, W. Maret, F. Chen, N. Tao, E. Forzani, *IEEE J. Transl. Eng. Health Med.* **2020**, *8*, 1–9.

[6] M. Tamura, K. Tokonami, Y. Nakagawa, K. Tomishige, *ACS Catal.* **2016**, *6*, 3600–3609.

[7] W. M. Czaplik, J. M. Neudörfl, A. J. von Wangelin, *Green Chem.* **2007**, *9*, 1163–1165.

[8] F. Alonso, P. Riente, M. Yus, *Acc. Chem. Res.* **2011**, *44*, 379–391.

[9] F. Alonso, P. Riente, M. Yus, *European J Org Chem* **2008**, 4908–4914.

[10] A. M. López-Vinasco, L. M. Martínez-Prieto, J. M. Asensio, P. Lecante, B. Chaudret, J. Cámpora, P. W. N. M. Van Leeuwen, *Catal. Sci. Technol.* **2020**, *10*, 342–350.

[11] F. Alonso, P. Riente, J. A. Sirvent, M. Yus, *Appl. Catal. A Gen.* **2010**, *378*, 42–51.

[12] F. Alonso, I. Osante, M. Yus, *Synlett.* **2006**, *2006*, 3017–3020.

[13] Y. Hu, Y. Yu, X. Zhao, H. Yang, B. Feng, H. Li, Y. Qiao, L. Hua, Z. Pan, Z. Hou, *Sci. China Chem.* **2010**, *53*, 1541–1548.

[14] K. P. Donegan, J. F. Godsell, D. J. Otway, M. A. Morris, S. Roy, J. D. Holmes, *J. Nanoparticle Res.* **2012**, *14*, 670.

[15] N. J. S. Costa, M. Guerrero, V. Collière, É. Teixeira-Neto, R. Landers, K. Philippot, L. M. Rossi, *ACS Catal.* **2014**, *4*, 1735–1742.

[16] A. M. López-Vinasco, L. M. Martínez-Prieto, J. M. Asensio, P. Lecante, B. Chaudret, J. Cámpora, P. W. N. M. van Leeuwen, *Catal. Sci. Technol.* **2020**, *10*, 342–350.

[17] M. Cardona-Farreny, P. Lecante, J. Esvan, C. Dinoi, I. del Rosal, R. Poteau, K. Philippot, M. R. Axet, *Green Chem.* **2021**, *23*, 8480–8500.

[18] L. Zaramello, B. L. Albuquerque, J. B. Domingos, K. Philippot, *Dalton Trans.* **2017**, *46*, 5082–5090.

[19] C. Amiens, D. Ciuculescu-Pradines, K. Philippot, *Coord. Chem. Rev.* **2016**, *308*, 409–432.

[20] H. yan Jiang, S. shi Zhang, B. Sun, *Catal. Lett.* **2018**, *148*, 1336–1344.

[21] P. Migowski, G. Machado, S. R. Texeira, M. C. M. Alves, J. Morais, A. Traverse, J. Dupont, *Phys. Chem. Chem. Phys.* **2007**, *9*, 4814–4821.

[22] M. H. G. Prechtl, P. S. Campbell, J. D. Scholten, G. B. Fraser, G. Machado, C. C. Santini, J. Dupont, Y. Chauvin, *Nanoscale* **2010**, *2*, 2601.

[23] H. Konnerth, M. H. G. Prechtl, *Chem. Commun.* **2016**, *52*, 9129–9132.

[24] H. Konnerth, M. H. G. Prechtl, *New J. Chem.* **2017**, *41*, 9594–9597.

[25] K. Vijayakrishna, K. T. P. Charan, K. Manojkumar, S. Venkatesh, N. Pothanagandhi, A. Sivaramakrishna, P. Mayuri, A. S. Kumar, B. Sreedhar, *ChemCatChem* **2016**, *8*, 1139–1145.

[26] R. Mariappan, S. Mahalingam, *Asian J. Chem.* **2013**, *25*, 3081–3083.

[27] J. He, L. Schill, S. Yang, A. Riisager, *ACS Sustain. Chem. Eng.* **2018**, *6*, 17220–17229.

[28] J. He, M. R. Nielsen, T. W. Hansen, S. Yang, A. Riisager, *Catal. Sci. Technol.* **2019**, *9*, 1289–1300.

[29] F. A. Harraz, S. E. El-Hout, H. M. Killa, I. A. Ibrahim, *J. Catal.* **2012**, *286*, 184–192.

[30] Z. Sun, Y. Wang, M. Niu, H. Yi, J. Jiang, Z. Jin, *Catal. Commun.* **2012**, *27*, 78–82.

[31] W. Zhu, H. Yang, Y. Yu, L. Hua, H. Li, B. Feng, Z. Hou, *Phys. Chem. Chem. Phys.* **2011**, *13*, 13492–13500.

[32] F. A. Harraz, S. E. El-Hout, H. M. Killa, I. A. Ibrahim, *J. Mol. Catal. A Chem.* **2013**, *370*, 182–188.

[33] D. Krishnan, L. Schill, M. R. Axet, K. Philippot, A. Riisager, *Nanomaterials* **2023**, *13*, 1459.

[34] M. Yang, P. S. Campbell, C. C. Santini, A. V. Mudring, *Nanoscale* **2014**, *6*, 3367–3375.

[35] H. W. Nesbitt, D. Legrand, G. M. Bancroft, *Phys. Chem. Miner.* **2000**, 27, 357–366

[36] P. Prieto, V. Nistor, K. Nouneh, M. Oyama, M. Abd-Lefdil, R. Díaz, *Appl. Surf. Sci.* **2012**, *258*, 8807–8813.

[37] J. Li, P. Li, J. Li, Z. Tian, F. Yu, *Catalysts* **2019**, *9*, 506.

[38] J. Liu, Y. Zhu, C. Wang, T. Singh, N. Wang, Q. Liu, Z. Cui, L. Ma, *Green Chem.* **2020**, *22*, 7387–7397.

[39] L. Qin, S. H. Lee, K. H. Kim, O. Lun Li, *Appl. Surf. Sci.* **2022**, *587*, 152849.

[40] S. Chen, C. Ciotonea, A. Ungureanu, E. Dumitriu, C. Catrinescu, R. Wojcieszak, F. Dumeignil, S. Royer, R. Wojcieszak, *Catal. Today* **2019**, *334*.

[41] S. Song, S. Yao, J. Cao, L. Di, G. Wu, N. Guan, L. Li, *Appl. Catal. B* **2017**, *217*, 115–124.

[42] K. Philippot, A. Roucoux, *Nanoparticles in Catalysis: Advances in Synthesis and Applications,* VCH, Weinheim, **2021**, p. 73–97.

[43] Y. Hu, Y. Yu, Z. Hou, H. Yang, B. Feng, H. Li, Y. Qiao, X. Wang, L. Hua, Z. Pan, X. Zhao, *Chem. Asian J.* **2010**, *5*, 1178–1184.

[44] F. Alonso, P. Riente, M. Yus, *Tetrahedron* **2009**, *65*, 10637–10643.

Entry for the Table of Contents

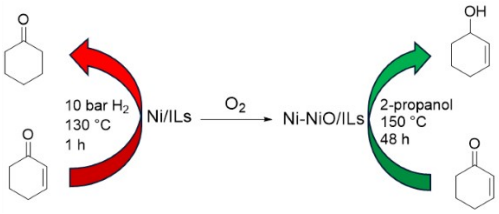

Nanocatalyst systems with Ni nanoparticles in functionalized ionic liquids (Ni/ILs) exhibits good catalytic activity for the chemoselective hydrogenation of 2-cyclohexen-1-one to cyclohexanone under relatively mild reaction conditions. Conversely, after aerobic oxidization the resulting Ni-NiO/ILs systems were active for selective catalytic transfer hydrogenation (CTH) of 2-cyclohexen-1-one to 2-cyclohexen-1-ol with 2-propanol, also under mild reaction conditions.